Temperature rise in mass concrete elements – model development and experimental verification using concrete at Katse Dam

TECHNICAL PAPER
Journal of the South African Institution of Civil Engineering, 46(1) 2004, Pages 9–14, Paper 565

Y Ballim

This paper describes the development, operation and experimental verification of a finite difference heat model for predicting the time-based temperature profiles in large concrete elements. The model represents a two-dimensional solution to the Fourier heat flow equation and can be implemented in a commercially available spreadsheet package.

The proposed model uses the rate of internal heat evolution, determined from an adiabatic calorimeter, as input. This approach allows the model to use the heat rate of the actual concrete to be used in the structure. A further development is that the model uses a maturity function, rather than clock time, to describe the rate of heat development as well as the distribution of this rate over time or extent of hydration of the cement.

The paper also presents the results of a verification exercise which was conducted during the construction of the Katse Dam in Lesotho. An 8 m³ block of concrete was cast and instrumented to monitor temperatures at various positions in the block over approximately nine days after casting. The results show that the proposed model is able to predict the temperature at internal points in the concrete block to within 2 °C of the measured values.

YUNUS BALLIM obtained his BSc (Civil Eng), MSc (Civil Eng) and PhD degrees from the University of the Witwatersrand (Wits) in 1981, 1983 and 1994 respectively. He worked for D&H Construction on road and bridge projects, followed by three years in the precast concrete industry with Vianini Pipes (Pty) Ltd and Fraser Fyfe (Pty) Ltd as technical manager and later as non-executive member of the Board of Directors. In 1989 he was awarded the Portland Cement Institute Research Fellowship based at the Department of Civil Engineering at Wits. In 1992, he was appointed as a lecturer in the Department of Civil Engineering at Wits. Since 2001, he has been the head of the School of Civil & Environmental Engineering.

Keywords: mass concrete; hydration; temperature; maturity; finite difference; heat modelling; adiabatic calorimetry

INTRODUCTION

The hydration of cement is an exothermic reaction that produces substantial amounts of heat. In concrete construction involving relatively small elements, this heat energy is quickly dissipated to the environment and this usually poses no serious problems. However, in large or mass concrete elements, thermally induced cracking is a problem requiring special attention at the design and construction stages. The form of variation in thermally induced stress at typical surface and internal points in the concrete is illustrated in figure 1. During the early stages, when the internal temperature of the immature concrete is increasing, the cooler surface zone (point A) is subjected to tensile stresses and surface cracks, usually fairly shallow, occur within a few days after casting. At later ages, after the peak temperature has been reached and the internal concrete enters the cooling phase, the increased stiffness of the surface zone now acts as a restraint to the thermal shrinkage of the internal concrete. Internal sections (point B) are therefore subjected to tensile stresses and significant internal cracking is possible during this period. During this phase, the surface sections experience a compressive stress regime.

Whether or not the concrete will crack in response to these applied stresses depends on a wide range of interconnected intrinsic and extrinsic factors (Andersen 1998). Of these, a fundamental factor is the time-based temperature profiles in the concrete structure. An accurate and thorough understanding of the temperature differences occurring in the concrete at different times (as the physical properties change and evolve) is essential for a proper analysis of the cracking potential. Furthermore, from a practical point of view, a temperature prediction model is also necessary for the design and planning of cooling systems in the concrete as well as to give the contractor an indication of the likely times when grouting of joints can be undertaken.

This paper discusses the development of a finite difference (FD) numerical model for predicting the temperature at varying times and locations in a mass concrete element. The model is applicable to a rectangular concrete element, which is typical of the construction of large concrete structures such as dams and foundations. The model is a two-dimensional solution of the Fourier equation for heat flow in solid bodies and, as presently structured, is simple enough to be programmed into a commercially available spreadsheet package.

An important problem facing heat modelling of concrete is that the rate of heat evolution at any point in the concrete element is dependent on the specific binder and aggregate type and mixture proportions used in the concrete as well as the degree of hydration at each point in the element at a particular time under consideration. The present model resolves much of this complexity by incorporating the results of a rate of heat evolution determination using a low-cost adiabatic calorimeter. A small sample of the actual con-

crete used in the element is placed in the calorimeter and the temperature rise is monitored over a period of approximately seven days. These results are then used to determine the rate of heat evolution and the time scale is converted to a maturity scale to indicate the extent of hydration. The finite-difference model uses this form of the results to determine the rate of heat evolution at various times and locations in the structural element, and hence determine the temperature profiles in the element.

Finally, the paper presents the results of a verification exercise that was carried out to assess the accuracy of the model. An 8 m³ block of concrete was cast on site during the construction of the Katse Dam on the Lesotho Highlands Water Project. This block was instrumented with thermal probes and the temperature at various points in the block was monitored over approximately 200 hours after casting.

DEVELOPMENT OF THE HEAT MODEL

The flow of heat in concrete is governed by the Fourier equation which, in its two-dimensional transient form, can be expressed as:

$$\rho C_p \frac{\partial T}{\partial t} = k\left(\frac{\partial^2 T}{\partial x^2} + \frac{\partial^2 T}{\partial y^2}\right) + \dot{q}_t \qquad (1)$$

where: ρ = density of the concrete; C_p = specific heat capacity of the concrete; T = temperature; t = time; k = thermal conductivity of the concrete; x, y, are the coordinates at a particular point in the structure; and $\dot{q}_t$ = rate of internal heat evolution, which varies over time.

Equation 1 was solved numerically for a rectangular block of concrete that has a z dimension significantly larger that the x and y dimensions. As shown in figure 2, the block is cast onto a rock foundation and the ambient temperature (T_A) varies with time.

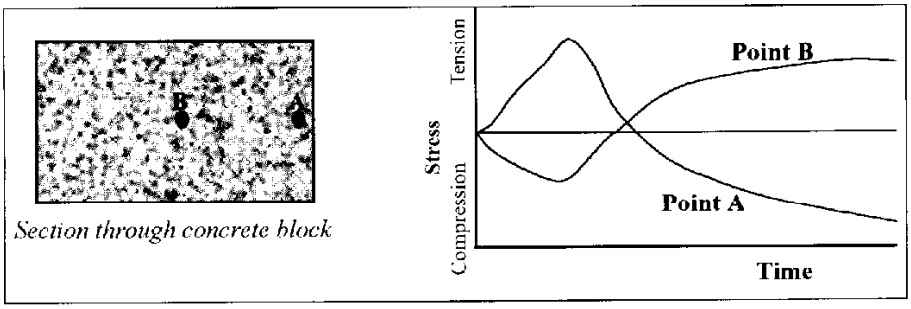

Figure 1 Illustration of the variation of stress at two points in an internal section of a mass concrete element

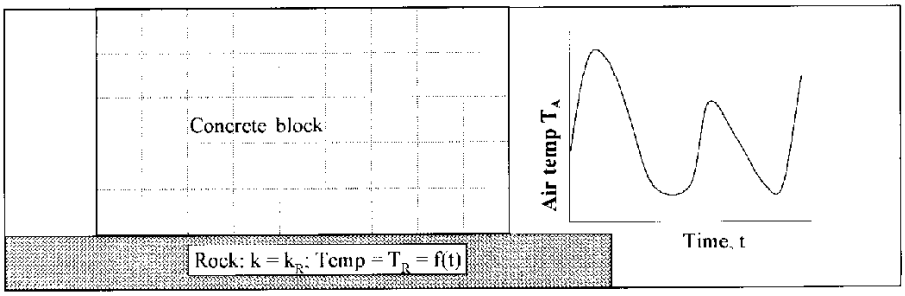

Figure 2 Schematic arrangement of the modelled mass concrete block

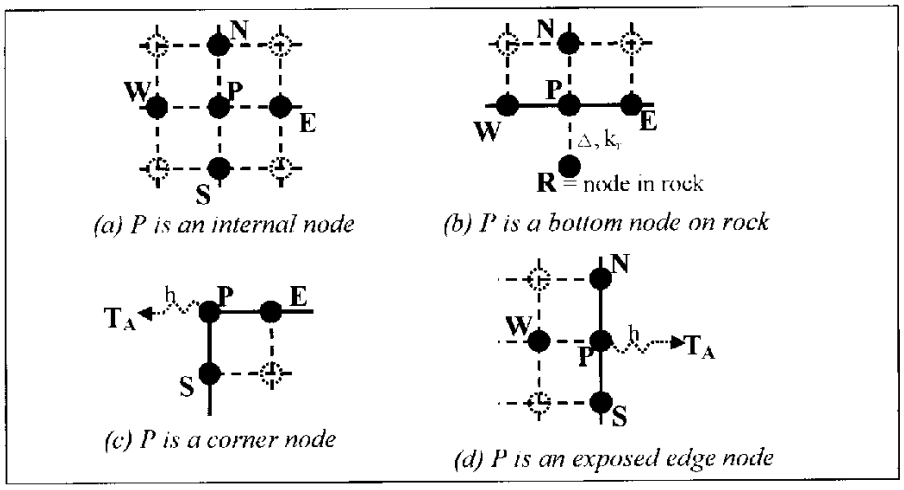

Figure 3 Node positions and boundaries for which FD equations were set up

The numerical solution of equation 1 is covered in a number of texts (Holman 1990; Dusinberre 1961; Croft & Lilley 1977) and only the final form of the finite difference equations for the different nodal positions in the concrete block and associated boundary conditions will be presented here. Figure 3 shows the different node positions for which the finite difference equations were developed.

Internal nodes (refer to figure 3(a))

The FD equation for this type of node is given as:

$$T_P^{n+1} = \frac{\dot{q}_t^n \delta t}{\rho C_p} + T_P^n(1-4F_o) + F_o(T_N^n + T_E^n + T_S^n + T_W^n) \qquad (2)$$

subject to:

$$\delta t \le \frac{\rho C_p \Delta^2}{4k} \qquad (3)$$

where, (further to the parameters defined before): T_X^n is the temperature at node X in the nth time interval; $\dot{q}_t^n$ is the time-rate of heat evolution from the hydrating cement during the n^{th} time interval; δt is the time-step interval used in the FD analysis; C_p is the specific heat capacity of the concrete, determined as the mass weighted average of the individual specific heat capacity of each component in the mix (Addis 1986); F_o is the Fourier number which is defined as:

$$F_o = \frac{k\delta t}{\rho C_p \Delta^2} \qquad (4)$$

and $\Delta = \Delta_X = \Delta_Y$ is the distance between nodes. The limitation on δt in equation 3 is so as to ensure stability of the FD model.

Bottom surface nodes (refer to figure 3(b))

A fictitious node R is included in the system at a distance Δ from P and the thermal conductivity of the rock is k_R. The governing equation is then of the form:

$$T_P^{n+1} = \frac{\dot{q}_t^n \delta t}{\rho C_p} + T_P^n\left[1 - F_o\left(4 + 2\frac{k_R}{k}\right)\right] + F_o\left(2T_N^n + T_E^n + T_W^n + 2\frac{k_R}{k}T_R^n\right) \qquad (5)$$

subject to:

$$\delta t \le \frac{\rho C_p \Delta^2}{k\left(4 + 2\frac{k_R}{k}\right)} \qquad (6)$$

In the absence of direct solar radiation, the temperature response of materials like rock, to variations in the ambient temper-

ature, is slow. The temperature of the rock at node R, T_R^n, is therefore taken as the minimum temperature occurring on the previous day.

Corner nodes (refer to figure 3(c))

In this case, heat is also transferred between node P and the environment by conduction and the rate of such transfer is determined by the heat transfer coefficient h. The governing equation is then of the form:

$$T_P^{n+1} = \frac{\dot{q}_t^n \delta t}{\rho C_p} + T_P^n\left[1 - 4F_o\left(1 + B_i\right)\right] + 2F_o\left(T_S^n + T_E^n + 2B_i T_A^n\right) \quad (7)$$

subject to:

$$\delta t \le \frac{\rho C_p \Delta^2}{4k\left(1 + B_i\right)} \quad (8)$$

where T_A is the ambient temperature and B_i is the Biot number which is defined as:

$$B_i = \frac{h\Delta}{k} \quad (9)$$

Exposed surface nodes (refer to figure 3(d))

As for the corner nodes, heat is transferred to the environment and the FD equation is:

$$T_P^{n+1} = \frac{\dot{q}_t^n \delta t}{\rho C_p} + T_P^n\left[1 - 4F_o\left(1 + \frac{B_i}{2}\right)\right] + F_o\left(2T_W^n + T_S^n + T_N^n + 2B_i T_A^n\right) \quad (10)$$

subject to:

$$\delta t \le \frac{\rho C_p \Delta^2}{\left(4k + 2h\Delta\right)} \quad (11)$$

In the operation of the numerical model, the time step interval (δt) has to be selected so as to be less than the minimum value determined from equations 3, 6, 8 and 11.

Modelling the environmental temperature T_A

At the design stage of a construction project, it is unlikely that reliable and continuous ambient temperature values are available for the area in which the construction is to take place. This is more so because temperature values are required at approximately one-hour intervals. However, daily ambient maximum and minimum temperatures are usually easily available from the local meteorological office and a model was developed to predict the ambient temperature at any time using only the daily maximum and minimum values. This model takes the form:

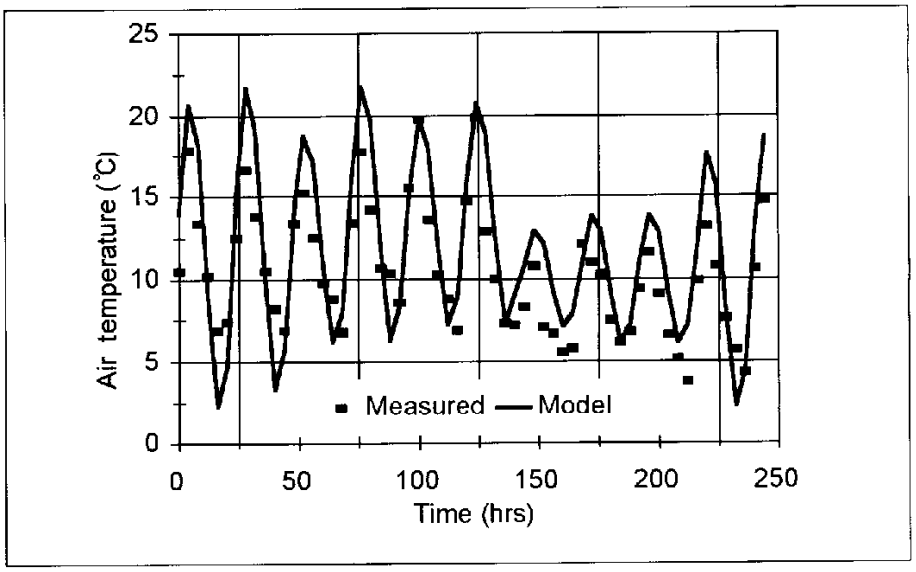

Figure 4 Measured air temperature compared to the modelled values using equation 12

$$T_A = -\sin\left(\frac{2\pi\left(t_d + t_m\right)}{24}\right)\left(\frac{T_{max} - T_{min}}{2}\right) + \left(\frac{T_{max} + T_{min}}{2}\right) \quad (12)$$

where: t_d is the clock time of day at which the prediction is being made (0 to 24 hours); t_m is the time at which the minimum overnight temperature occurs (usually just at sunrise); T_{max} and T_{min} are respectively the maximum and minimum temperatures for the day under consideration.

The model is fairly rough in that it ignores factors such as cloud cover, wind or direct sunlight and there is probably room for significant refinement. Nevertheless, figure 4 shows that the model gives reasonably good prediction when compared with actual measured outdoor temperatures over a period of approximately ten days. In developing figure 4, temperatures were measured at random times at the concrete mixing area on a construction site over the period shown. The site also had a maximum and minimum temperature recording system and these results were used in equation 12 to develop the modelled results.

Determining the rate of internal heat evolution, $\dot{q}_t$

An adiabatic calorimeter was developed and built to measure the rate of heat evolution of a concrete mixture to be used in the construction of the concrete element. Details of the construction and operation of the calorimeter are given by Gibbon *et al* (1997) and Gibbon and Ballim (1996). In principle, the test involves placing a one-litre sample of concrete in a water bath, such that a stationary pocket of air separates the sample from the water. The signal from a thermal probe placed in the sample is monitored by a desktop computer and, via an input/output analogue to digital conversion card, the heater in the water bath is turned on and off so as to maintain the water at the same temperature as the concrete. This ensures that there is no exchange of heat between the concrete sample and the surrounding environment. The pocket of air around the sample is important to dampen out any harmonic response between the sample and water temperature as a result of the measurement sensitivity of the thermal probes. The test is usually run over a period of seven days, by which time the rate of heat evolution of the sample is too low to be detected as a temperature difference by the thermal probes – given that the thermal probes are accurate to approximately 0,5 °C.

The test produces a curve of temperature vs time for a particular binder type and mix composition. The total heat evolved at any time (q_t) can be determined from the relationship:

$$q_t = mC_p\delta T \quad (13)$$

where m is the mass of the sample and δT is the change in temperature of the sample over the time period under consideration. The rate of heat evolution is then determined from a numerical differentiation with respect to time (t) of the total heat curve, that is:

$$\dot{q}_t = \frac{\partial q_t}{\partial t} \quad (14)$$

However, equation 14 yields a rate of heat evolution that is unique to the conditions under which the adiabatic test was conducted. In determining the cumulative heat produced by the binder, equation 13 is only concerned with temperature differences and not absolute temperatures. As a chemical reaction, the rate and extent of hydration is influenced by the absolute temperature under which the reactions take place. In principle, therefore, each point in a concrete structure which is subjected to a unique time-tem-

perature profile will exhibit a unique heat rate curve.

Ballim and Graham (2002) have shown that approaches to the solution of equation 1 which consider the form of the time-based heat of hydration curve ($q_t = f(t)$) as constant (Clover 1937; Wang & Dilger 1994) are inappropriate, since they depend significantly on the test temperature conditions. In order to address this problem, Ballim and Graham (2002) propose that it is necessary to express the heat evolved, as measured in the adiabatic test, in terms of the a 'maturity heat rate' as a function of the cumulative maturity, rather than a time rate. The maturity heat rate ($\dot{q}_M = f(M)$ is expressed as:

$$\dot{q}_M = \frac{\partial q_t}{\partial M} \qquad (15)$$

where M is the maturity of the concrete expressed as the equivalent age of a concrete continuously cured at 20 °C. The equivalent age is calculated from the relative form of the Arrhenius relationship, which can be written as (Naik 1985):

$$t_{20} = \sum_{i=1}^{n} \exp\left[\left(\frac{E}{R}\right)\left(\frac{1}{273+T_o} - \frac{1}{T_i}\right)\right]\Delta t_i \qquad (16)$$

where t_{20} is the time required, when curing at 20 °C, to reach an equivalent maturity; T_i is the average concrete temperature (in K) in the time interval Δt_i; T_o is the reference temperature (taken as 20 °C); E is the apparent activation energy (taken as 33,5 kJ/mol (Bamford & Tipper 1969); R is the universal gas constant (8,31 J/mol.K).

The time-based heat rate, as required in equation 1, is then determined using the chain rule as follows:

$$\dot{q}_t = \dot{q}_M \cdot \frac{\partial M}{\partial t} \qquad (17)$$

The concrete temperature prediction model was therefore structured to use, as input, the calculated maturity and corresponding maturity heat rate determined from the adiabatic calorimeter test. It was also necessary for the model to maintain a measure of both the development of maturity (M) and the time-based rate of change of maturity ($\frac{\partial M}{\partial t}$) at each point under consideration in the concrete element.

Figure 5 shows the maturity-based rate of heat evolution of the concrete used in the verification exercise of this project (discussed later). The time axis is expressed in terms of t_{20} hours using equation 16. The curve was developed using the adiabatic calorimeter discussed above. In the operation of the heat model, the maturity heat rate curve, as in figure 5, is used as input data in its numerical form. At each time step in the analysis and at each discreet point in the structure, the cumulative maturity at that point is used to determine a corresponding maturity heat rate. This is then converted to a time-based heat rate for the particular time and position by multiplication by the rate of change of maturity at the position under consideration.

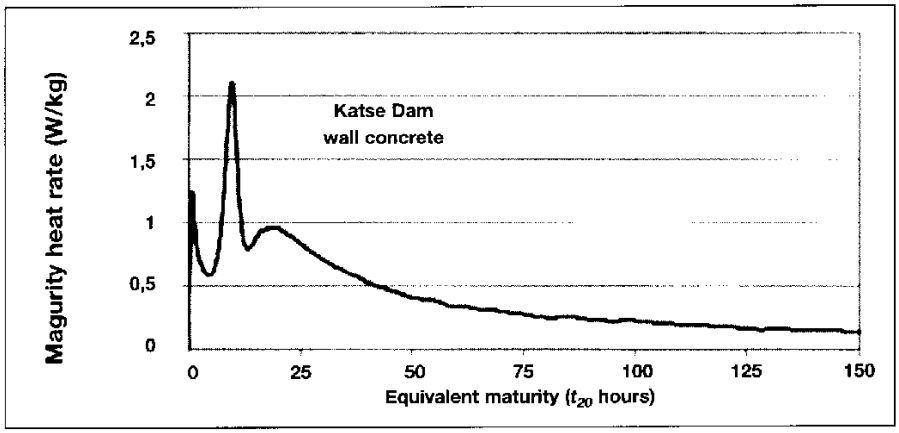

Figure 5 The maturity-based rate of heat evolution of a test concrete expressed in terms of the Arrhenius maturity function

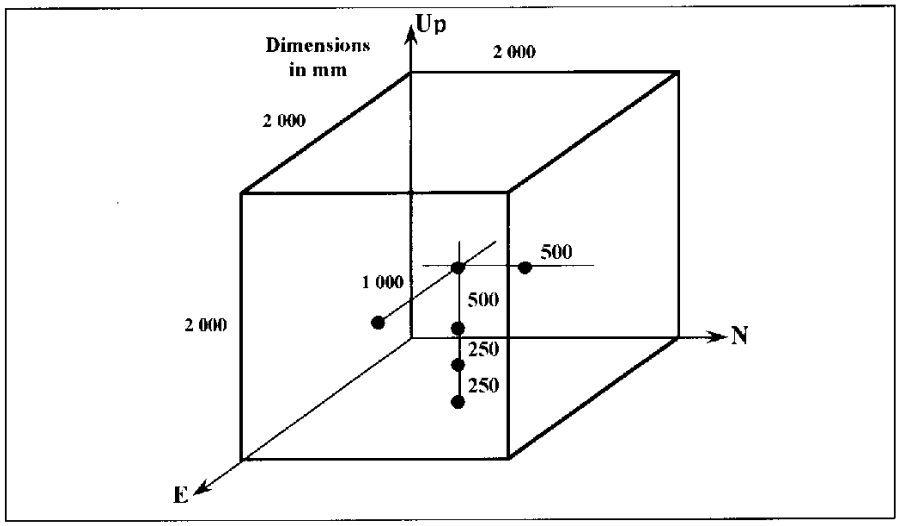

Figure 6 Position of temperature measurement probes in the concrete test block

Application of model to spreadsheets

With the increased sophistication of spreadsheet architecture and programming ability, it was found that the FD model could easily be programmed to run in a spreadsheet. The normal two-dimensional structure of a page and three-dimensional structure of a 'workbook' lends itself particularly well to the stepwise calculation requirements of the model. Also, the 'look-up' feature in these spreadsheets allows the user to install data sets of (say) heat rate and corresponding maturity. It is then possible to select appropriate values from the data set at each interval in the stepwise calculation. A similar procedure can be set up if the thermal conductivity of the concrete is known to vary with time and degree of hydration, as has been noted by some researchers (Van Breugel 1998).

LABORATORY VERIFICATION OF THE PROPOSED MODEL

An 8 m³ block of concrete, measuring 2 m x 2 m x 2 m, was cast on the concrete mixing platform of the Katse Dam construction site. The block was cast at some distance from the mixer plant but within reach of the overhead cable crane system which was used to transport materials and equipment onto the dam wall. Timber formwork was used to form the four vertical sides of the block and the concrete was cast directly onto the rock surface. Figure 6 shows the dimensions and orientation of the block, as well as the position of the six temperature measurement probes used.

Thermal probes were placed in the concrete at the node points shown in figure 6 and these were held in place by being tied to a network of thin fishing lines attached to the insides of the formwork. The probe in the centre of the east face of the block was placed at approximately 10 mm below the surface of the concrete. A probe was also placed on the outside of the concrete block to monitor the ambient temperature.

The thermal probes were manufactured using integrated circuit TO-92 Precision Centigrade temperature sensors that require a 5V dc power supply. These sensors were connected to doubly insulated

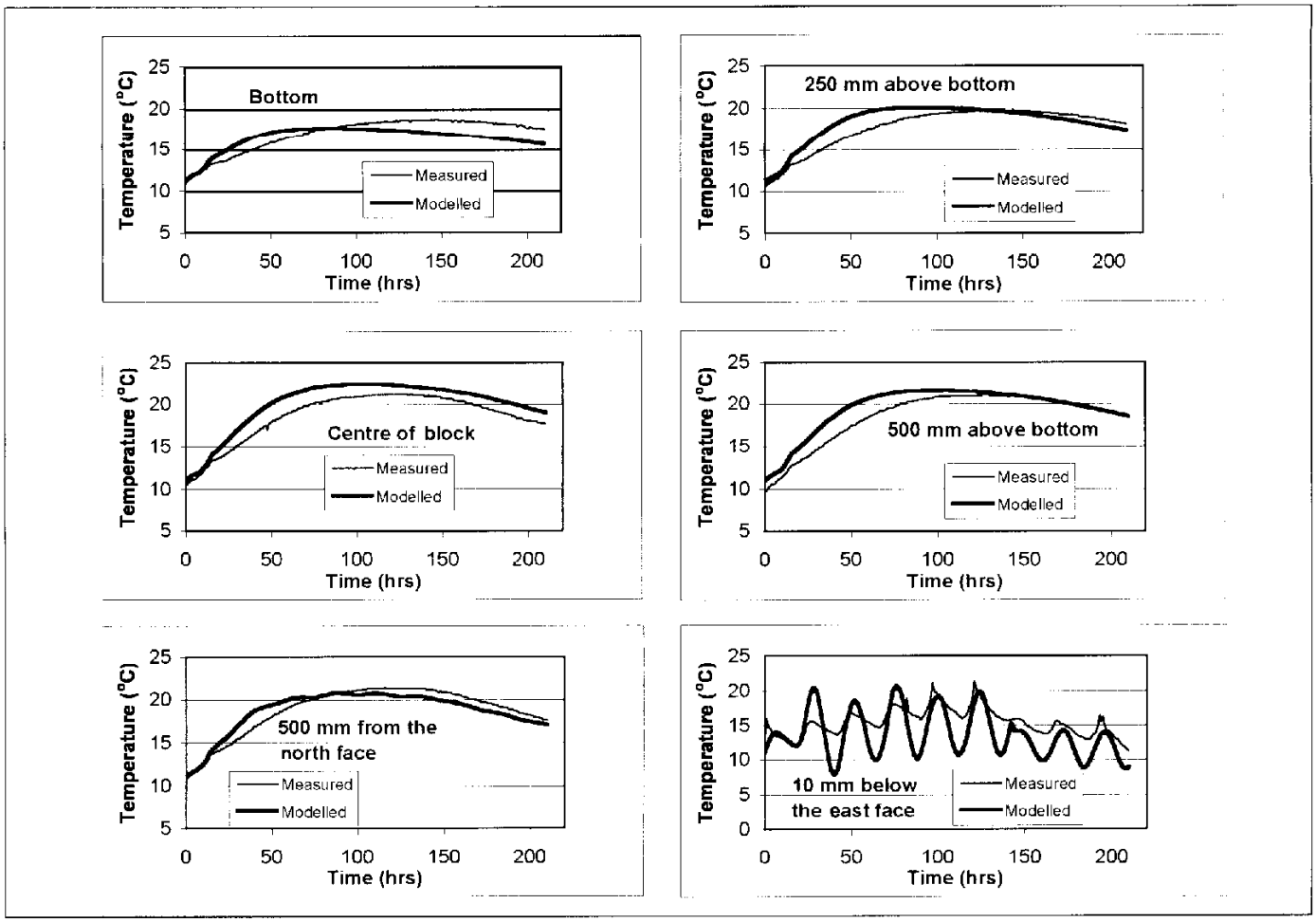

Figure 7 Measured and modelled temperatures at each of the node points indicated in figure 6

signal cable and the assembly was inserted into a 6 mm ϕ copper tube. The tubes were approximately 70 mm long, soldered at one end and sealed with heat shrink insulation at the other end. All the probes were calibrated against a glass calibration thermometer across a temperature range of 10 °C to 60 °C. It was found that none of the probes required a slope or offset correction as they all gave temperature readings which were within 0,2 °C of the glass thermometer readings.

The probes were connected to a read-only input card placed into an XT type personal computer. The computer and the constant power supply unit were placed in a lockable cabinet alongside the concrete block and the computer was set to record the signal from each probe in one-hour intervals.

Table 1 shows the mixture proportions of the concrete used to cast the test block. All the aggregates in the concrete were crushed doleritic basalt obtained from the on-site crushing plant. The use of crushed ice as part of the mixing water was aimed at reducing the placing temperature and, in the case of the test block, the placing temperature of the concrete was reduced to 11 °C. The concrete was sufficiently workable to be compacted with poker vibrators. However, in the vicinity of the temperature probes, concrete was carefully placed by hand and vibration was done in such a manner as to minimise bulk movement of the concrete in that area. The top of the concrete block was roughly finished and left uncovered. The side formwork was released at approximately 18 hours after casing.

Table 1 Mixture proportions (kg/m³) of the concrete used in the test block

Ordinary Portland Cement	154
Fly ash	66
Water	124
Crushed ice	35
Sand:	
• Fine	322
• Coarse	187
Stone:	
• 5 to 19 mm	321
• 19 to 38 mm	365
• 38 to 75 mm	472
• 75 to 150 mm	547
Water-reducing agent	0,7
Air-entraining agent	0,17

A sufficient quantity of each of the materials used in the concrete was obtained for the adiabatic calorimeter test. As the test sample is only approximately one litre in size, the aggregates larger than 19 mm were not included in the adiabatic test concrete. These fractions were replaced by an equal mass of the 5 to 19 mm size fraction. The results of this test, which were used as input for the FD model, are shown in figure 5. The thermal conductivity of the concrete was taken as 2,2 W/m.K (Van Breugel 1998), the specific heat was calculated to be 1158 J/kg.K (Addis 1986) and, using the range of values presented by Holman (1990), the heat transfer coefficient was taken as 26 W/m².K for exposed concrete surfaces and 5 W/m².K for surfaces covered by formwork over the first 18 hours after casting. The analysis was done in two-hour time steps with $\Delta x = \Delta y = 250$ mm.

RESULTS AND DISCUSSION

Figure 7 shows comparisons of the measured and modelled temperatures at each of the note points indicated in figure 6. The results show that the temperature of the concrete started at approximately 11 °C and reached a peak of 22 °C at the centre of the block. Depending on the position within the block the peak temperature occurred between 100 and 150 hours.

It is clear from figure 7 that the FD model predicts temperatures at internal points in the block to an accuracy of

approximately 2 °C. The exception occurred for nodes close to the surface where, for the monitoring period after release of the formwork, the model indicates a larger response to variation in ambient temperature than was actually measured at 10 mm below the surface. A possible reason for this is that some drying of the concrete occurred at the surface and this caused a reduction in the rate of hydration in this zone. Such drying would also have caused a reduction in the thermal conductivity of the concrete in the surface zone and this may explain the relative insensitivity of the concrete to variations in the ambient temperature.

Nevertheless, the inaccuracy of the model in predicting temperature at the surface of the concrete points to the importance, but also the complexity, of accurately defining the boundary conditions in the development of such a temperature model. As a case in point, the model described in this paper does not account for the effects of incident solar radiation, which can be very significant in southern Africa. However, to account for this parameter will mean different boundary conditions for the different surfaces of the concrete as well as a parameter to account for the effects of full or partial cloud cover. The effects of wind speed on the surface heat transfer coefficient adds further to this complexity.

It should be noted that the model prediction was also undertaken using a three-dimensional solution to the Fourier equation. However, this did not improve the accuracy of the prediction significantly. Such a result points to the significant thermal inertia of materials like concrete, where analysis in the third dimension is only justified for fairly small and slender sections.

Notwithstanding these observations, given the simplicity and low cost of the model and its operation, the results are promising. Further development of the model will focus on

- an improved definition of the boundary conditions to better account for the effects of construction methods and environmental conditions
- allowing for the effects of sequential construction – casting fresh concrete onto concrete from which all the heat has not yet been lost

Furthermore, using an ever-growing database of heat rate curves for different binder types, it is possible to assess the likely effects of different binder types on the temperature development within a particular concrete element for given environmental conditions. The model can therefore be used as a valuable tool in the selection of the concrete mix proportions before construction commences. The model can also be used to assess the efficacy of a reduced concrete mix temperature, which is normally achieved by using flaked ice as mix water or by injecting liquid nitrogen into the fresh concrete mix.

CONCLUSIONS

- The finite difference model described, together with the adiabatic calorimeter, provides a low-cost and reasonably accurate means for predicting the time-based temperature profiles in mass concrete structures where potential cracking may present a problem.
- At internal points in the concrete, the model is able to predict temperatures to within 2 °C of the measured temperatures.
- Early-age drying from the surface of the concrete and variations in the environmental conditions causes significant error in the modelled temperatures at the surface of the concrete.
- Further development of the model should be undertaken to better define the boundary conditions and to allow for the effects of sequential construction.

Acknowledgements

Sincere thanks are due to Mr A Benn for on-site assistance in arranging the instrumentation and casting of the test block as well as Dr G Gibbon for undertaking the adiabatic test of the concrete.

References

Addis, B J (ed) 1986. *Fulton's concrete technology.* 6th ed. Midrand: Portland Cement Institute.

Andersen, M E 1998. Design and construction of concrete structures using temperature and stress calculations to evaluate early-age thermal effects. *Materials science of concrete*, vol 5 (edited by J Skalny & S Mindess). American Ceramic Society, pp 191–263.

Ballim, Y & Graham, P C 2002. A maturity approach to the rate of heat evolution in concrete. *Magazine of Concrete Research*, 55(3):249–256.

Bamford, C H & Tipper C F H (eds) 1969. *The practice of kinetics. Comprehensive chemical kinetics.* Vol 1. London; Elsevier.

Clover, R E 1937. Calculation of temperature distribution in a succession of lifts due to release of chemical heat. *Journal of American Concrete Institute*, 34:105–116.

Croft, D R & Lilley, D G 1977. *Heat transfer calculations using finite difference equations.* London: Applied Science Publishers.

Dusinberre, G M 1961. *Heat transfer calculations by finite differences.* Pennsylvania: International Textbook Company.

Gibbon, G J & Ballim, Y 1996. Laboratory test procedures to predict the thermal behaviour of concrete. *Journal of the SA Institute of Civil Engineers*, 38(3):21–24.

Gibbon, G J, Ballim, Y & Grieve, G R H 1997. A low-cost, computer-controlled adiabatic calorimeter for determining the heat of hydration of concrete. *Journal of Testing and Evaluation* (ASTM), 25(2):261–266.

Holman, J P 1990. *Heat transfer.* 7th ed. New York: McGraw Hill.

Naik, T R 1985. Maturity functions for concrete cured during winter conditions. *Temperature effects on concrete*, ASTM STP 858 (edited by T R Naik). Philadelphia: American Society for Testing Materials, pp 107–117.

Van Breugel, K 1998. Prediction of temperature development in hardened concrete. In *Prevention of thermal cracking in concrete at early ages* (edited by R Springschmid). RILEM Report 15. London: E&FN Spon, pp 51–75.

Wang, C H & Dilger, W H 1994. Prediction of temperature distribution in hardening concrete. In *Thermal cracking in concrete at early ages* (edited by R Springschmid). London, E&FN Spon, pp 21–28.